JOURNAL OF MATERIALS SCIENCE 26 (1991) 2630–2636

Fracture toughness of liner board evaluated by the *J*-integral

B. S. WESTERLIND, L. A. CARLSSON*, Y. M. ANDERSSON
SCA Research, Box 3054, S-85003 Sundsvall, Sweden

The *J*-integral approach to characterizing the fracture toughness of liner board is investigated. Three methods, namely the single-specimen, multiple-specimen and Liebowitz non-linear energy method are evaluated in terms of accuracy and convenience in the fracture toughness determination. The multiple-specimen and Liebowitz methods yield consistent fracture toughness values that are independent of crack length, while the single-specimen method yields toughness values that depend on crack length. In terms of convenience the Liebowitz methods is superior to the multiple-specimen method since it requires fewer specimens and employs a data reduction methodology that is easily implemented.

1. Introduction

While linear elastic fracture mechanics serves as a useful tool for failure prediction for cracked or flawed bodies where the crack tip plastic region is small compared with the geometrical dimensions of the crack and the component [1, 2], it is now widely recognized that characterization of the in-plane fracture of paper necessitates the accommodation of plasticity effects around the crack tip [3–6]. The significant degree of yielding around the crack tip is, besides the inherent ductility of the cellulose fibres, due to the structure of the material as illustrated in Fig. 1. Extension of the crack necessitates consecutive fibre pull-outs and breakages which constitute a tortuous crack path. Furthermore, the thin sheet-like nature of paper promotes plane-stress rather than plane-strain conditions around the crack tip, which further enhances plastic deformation [1]. The large-scale yielding of the material around the crack tip causes non-linearities in the load–displacement record and the elastic stress intensity factor, κ, or the elastic strain energy release rate, G, become less meaningful measures of the fracture toughness.

The *J*-integral [7] has been proposed by several authors as a parameter to measure the crack tip elastic–plastic field. The fracture criterion is stated so that crack extension occurs when J reaches its critical value J_c [8]. A major reason for the popularity of the *J*-integral is that it is readily evaluated from the global load–displacement record. The classical approach to experimentally determining the *J*-integral is to analyse load–displacement curves of identical specimens with varying crack lengths [8]. This method (multiple specimen) will be described in detail in a later section and examined experimentally.

To avoid the substantial experimental effort required for the multiple-specimen approach, Rice *et al.* [9] proposed a separation of elastic and plastic energy that enables the critical value of the *J*-integral to be established from testing a single specimen. Steadman and Fellers [4], however, found that the single-specimen method of Rice *et al.* [9] did not produce consistent values of the fracture toughness J_c of sack-paper. This will be further investigated below.

As early as 1971, Liebowitz and Eftis [10] derived a non-linear fracture toughness parameter, $\tilde{G}_c$, from a Ramberg–Osgood type of description of the non-linear load–displacement curve. This method has many similarities with the *J*-integral definition which

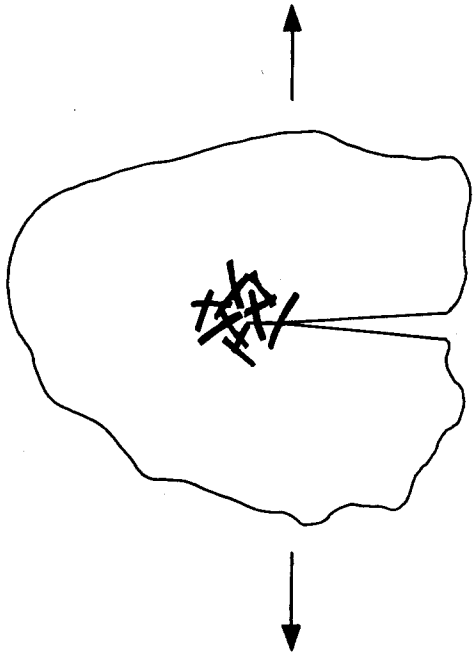

Figure 1 Crack extension in paper.

* *Permanent affiliation*: Florida Atlantic University, Department of Mechanical Engineering, Boca Raton, Florida 33431, USA.

0022–2461/91 $03.00 + .12

was recognized by Eftis *et al.* [11] and verified experimentally for various metal alloys by Poulose *et al.* [12]. To our knowledge a comparison between the non-linear fracture energy method of Liebowitz and Eftis [10] and the multiple- and single-specimen methods as applied to the fracture of paper has not been presented.

It is the purpose of this study to examine these methods in terms of their ability to measure the fracture toughness of liner board in the most consistent and convenient way.

2. Determination of *J*-integral

For Mode I fracture characterization of paper a centre-notched (CEN) specimen has been found adequate [4] (Fig. 2). Fig. 3 schematically illustrates load–displacement records for CEN specimens at crack lengths $2a$ and $2(a + \Delta a)$, respectively. As discussed by Begley and Landes [8] the J-integral for an elastic–plastic material can be expressed as

$$J = -\Delta U/t\Delta a \quad (1)$$

where ΔU is the change in potential energy upon crack extension (shaded area in the load–displacement diagram in Fig. 3), t is the specimen thickness and Δa is the incremental crack extension.

The rough surface and porous structure of paper make it difficult to define and measure the thickness without a certain degree of arbitrariness [13]. For this reason it is common to define a fracture parameter that does not require a measurement of thickness. Such a parameter is simply obtained as

$$J^* = tJ/w = J/\rho \quad (2)$$

where t is the thickness, w is the areal weight (grammage) and ρ is the density of the material. The critical value of J^* may thus be considered as a specific fracture energy of the material.

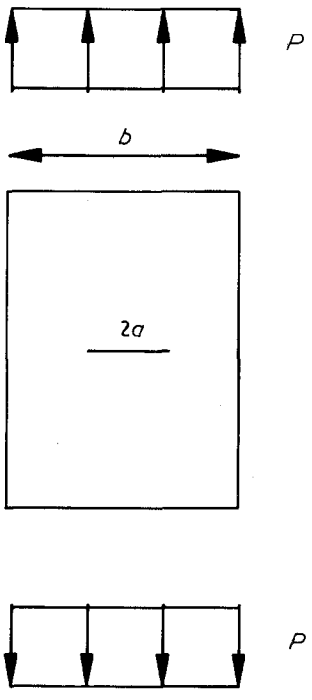

Figure 2 Centre notch specimen (CEN).

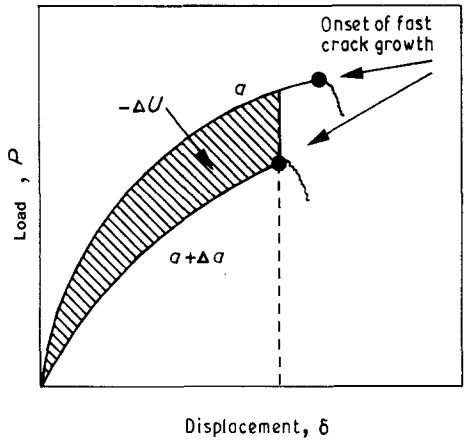

Figure 3 Load–displacement curves for specimens having crack lengths of a and $a + \Delta a$.

To determine the critical value of J^*, J_c^*, three methods discussed in the introduction will be examined, namely the multiple-specimen technique (MST), the single-specimen technique (SST) and the Liebowitz non-linear technique (LNT).

2.1. Multiple-specimen technique (MST)

The MST is based on a straightforward application of Equation 1. A set of CEN specimens with various crack lengths are prepared and loaded to fracture as indicated in Fig. 3. To achieve confidence in the load–displacement curve a large number of test specimens is required (typically more than 10 for paper) for each crack length. Once the load–displacement curve has been established with enough confidence for each crack length, the shaded area (corresponding to ΔU in Equation 1) in graphs similar to Fig. 3 is integrated numerically as a function of the displacement δ. The critical value of $J = J_c$ is established at the critical displacement for crack growth, $\delta = \delta_c$. Fig. 4 shows a representative actual load–displacement curve for a 200 g m^{-2} liner board CEN specimen. It is observed that the initiation of slow crack growth (marked with

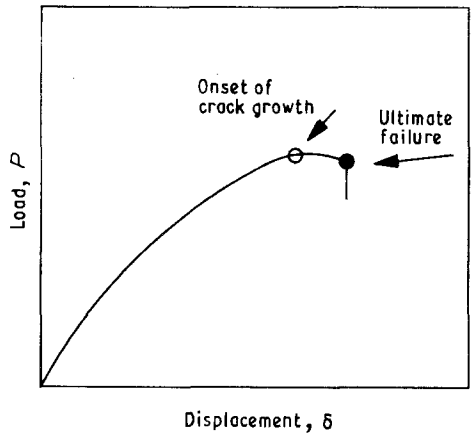

Figure 4 Typical load–displacement curve for CEN liner board specimen (200 g m^{-2}) in the CD. Stable crack extension is commonly observed prior to fracture.

an open circle) corresponds to a discontinuity in the load–displacement record which occurs close to the ultimate load. In tough papers it is difficult to observe this discontinuity in the load–displacement graph, and only the fracture toughness corresponding to catastrophic fracture (marked by the solid circle in Fig. 4) is evaluated. The J_c^* value so determined corresponds to the fracture energy for fast (critical) crack propagation.

2.2. Single-specimen technique (SST)

This method was proposed by Rice *et al.* [9] as an alternative to the MST discussed above. In contrast to the extensive testing and data reduction required for the MST, the J_c^* determination only requires one crack length. The method is based on separation of the elastic and plastic parts of the J-integral,

$$J = J_e + J_p \tag{3}$$

The elastic component of J is equal to the elastic strain energy release rate, G; $J_e = G$ where G is given by [14]

$$G = \frac{\kappa^2}{(2E_xE_y)^{1/2}}\left[\left(\frac{E_x}{E_y}\right)^{1/2} - \nu_{xy} + \frac{E_x}{2G_{xy}}\right]^{1/2} \tag{4}$$

where κ is the stress intensity factor [1],

$$\kappa = \sigma(\pi a)^{1/2}[\cos(\pi a/b)]^{-1/2} \tag{5}$$

in which σ is the far-field stress, $\sigma = P/bt$, a is half the crack length and b is the width of the CEN specimen [1]. E_x, E_y and G_{xy} are the Young's moduli in the loading direction, and transverse to the loading direction and the in-plane shear modulus, respectively. ν_{xy} is Poisson's ratio for loading in the x direction.

The plastic component of the J-integral for a CEN specimen tested in displacement control is, according to Rice *et al.* [9],

$$J_p = \frac{1}{t(b-2a)}\left(2\int_0^{\delta_p} P\,d\delta_p - P\delta_p\right) \tag{6}$$

where δ_p is the plastic component of the total displacement. Following Uesaka [3], the quantity inside the brackets in Equation 6 is identified as twice the shaded area A in Fig. 5. To obtain the specific fracture energy,

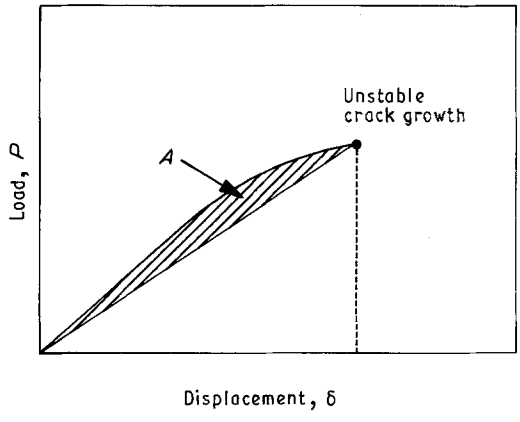

Figure 5 Schematic load–displacement curve for a notched specimen. Shaded area is proportional to the plastic component of the J-integral according to the single-specimen method.

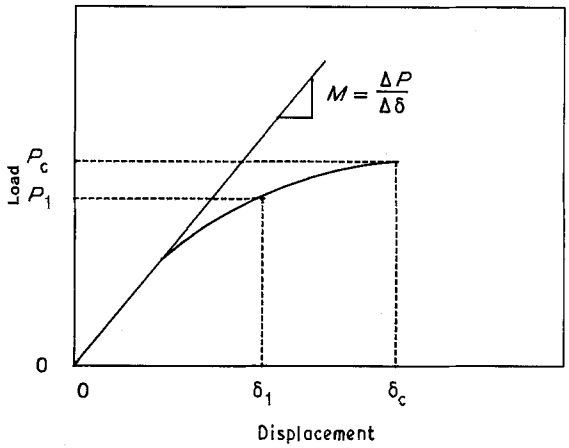

Figure 6 Schematic load–displacement curve for a notched specimen. M is the initial slope of the curve and (P_c, δ_c) and (P_1, δ_1) are two arbitrarily chosen points on the non-linear part of the curve.

J_c^*, J defined by Equation 3 is simply multiplied by thickness and divided by areal weight (Equation 2).

2.3. Liebowitz non-linear technique (LNT)

As discussed in the introductory section, Liebowitz and co-workers [10–12] proposed a non-linear fracture energy, $\tilde{G}_c$, which by similarity of definition may be used for J_c determination. The method is based on a Ramberg–Osgood description of the non-linear load–displacement (P–δ) curve:

$$\delta = \frac{P}{M} + k\left(\frac{P}{M}\right)^n \tag{7}$$

where the parameters k and n characterize the deviation from non-linearity and M is the initial stiffness of the CEN specimen.

To determine the parameters k and n in Equation 7 two points, (P_1, δ_1) and (P_c, δ_c), on the non-linear part are selected (Fig. 6). Substitution of these values into Equation 7 leads to a system of two equations. Solving these equations simultaneously provides the unknowns k and n. Based on Equation 7 Liebowitz and co-workers [10, 11] derived a non-linear correction factor β to the elastic energy release rate G and obtained

$$J \approx \tilde{G} = (1+\beta)J_e \tag{8}$$

At the point of fast fracture, $P = P_c$ and $J = J_c$, and

$$\beta = \frac{2nk}{n+1}\left(\frac{P_c}{M}\right)^{n-1} \tag{9}$$

Again, the specific fracture energy J_c^* is calculated from Equation 2.

3. Experimental procedure

3.1. Mechanical properties

Two commercially available liner boards manufactured by SCA (Munksund, Sweden) were selected. Areal weights (grammage) and mechanical properties were determined according to standard test procedures and are provided in Table I.

TABLE I Mechanical properties of kraft liner[a]

Grammage ($g\,m^{-2}$)	Thickness (mm)	S_T^{MD} ($MN\,m^{-1}$)	S_T^{CD} ($MN\,m^{-1}$)	X_T^{MD} ($kN\,m^{-1}$)	X_T^{CD} ($kN\,m^{-1}$)	ε_T^{MD} (%)	ε_T^{CD} (%)
200	0.264	1.70 ± 0.03	0.61 ± 0.01	18.0 ± 1.0	7.60 ± 0.2	1.8 ± 0.2	4.8 ± 0.2
400	0.508	2.92 ± 0.04	1.11 ± 0.01	35.4 ± 1.3	14.9 ± 0.3	2.3 ± 0.2	5.0 ± 0.3

[a] Mean values and 95% confidence limits based on ten replicates are listed. S_T = tensile stiffness, X_T = tensile strength, ε_T = ultimate strain in tension, MD = machine direction, CD = cross direction.

3.2. Fracture testing

A universal tensile tester (Alwetron TCT 10) was employed in the fracture tests performed at a cross-head speed of 1 cm min^{-1} and at a test section length of 15 cm.

Thin sheet-like specimens show a tendency to buckle out of plane in the cracked region because of a non-uniform Poisson contraction. In order to prevent buckling, supports were fitted to the specimens as illustrated in Fig. 7. To minimize friction a Teflon (PTFE) plate of dimensions 15 cm × 8 cm × 1 cm (length × width × thickness) was connected to a 5 cm × 8 cm × 1 cm (length × width × thickness) polycarbonate (PC) plate by means of two centrally located spring-loaded screws (see Fig. 7).

To evaluate the fracture toughness J_c^*, CEN specimens with cracks of lengths ($2a$) of 1, 2 and 3 cm were cut with razor blades of length identical to the crack length. Normally ten specimens were tested and an average curve from these tests was used to calculate the fracture toughness. Six specimens in the machine and cross directions (MD and CD) for the 200 $g\,m^{-2}$ board were used to evaluate the influence of the normal force in the anti-buckling supports (Fig. 7) on the load–displacement response.

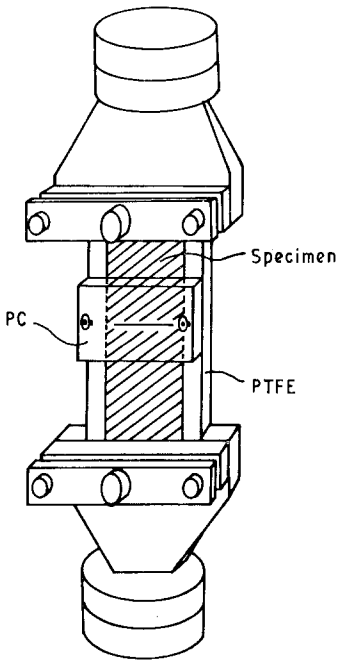

Figure 7 Schematic of anti-buckling supports for fracture tests of CEN specimens.

4. Results and discussion

4.1. Evaluation of anti-buckling supports

Ideally the anti-buckling supports would provide resistance only to lateral displacements of the paper. However, due to friction the normal pressure exerted on the paper over the area of the supports may provide resistance also to axial deformation in the cracked region. To examine the influence of normal pressure on the load–displacement curve, zero, low and high pressures were applied. The clamping force was not measured directly. However, the frictional force required to pull a specimen through the supports was recorded and found to be about 3 and 11 N for low and high clamping pressure, respectively.

Fig. 8 shows load–displacement curves for 200 $g\,m^{-2}$ liner board CEN specimens loaded in the MD without supports and with low and high clamping force in the supports. The three upper curves (1 to 3) represent a normalized crack length ($2a/b$) of 0.4, while the three lower curves (4 to 6) represent $2a/b = 0.6$. Each curve represents an average from three replicates. Inspection of the curves shows that unsupported CEN specimens fail at low loads in relation to the supported ones. Buckling of the material around the crack tip evidently enhances the stress intensity, resulting in the observed decrease of ultimate load.

The anti-buckling supports provide more even loading of the specimen, resulting in an increase in the failure load that is far more than could be accounted

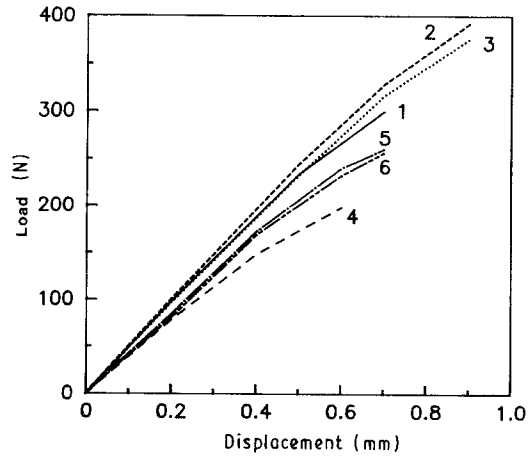

Figure 8 Influence of pressure in anti-buckling supports on load–displacement curves for kraft liner (200 $g\,m^{-2}$) in the MD. (1) $2a/b = 0.4$, no supports; (2) $2a/b = 0.4$, low pressure; (3) $2a/b = 0.4$, high pressure; (4) $2a/b = 0.6$, no supports; (5) $2a/b = 0.6$, low pressure; (6) $2a/b = 0.6$, high pressure.

for by friction. In fact, the curves for low and high contact pressure are virtually identical for both crack lengths, indicating that friction is not a major factor. In the remainder of this study low contact pressure was applied.

4.2. Crack sensitivity

The sensitivity of a material to cracks may be illustrated by a simple net strength concept. By considering Fig. 2 it is easily recognized that a material completely insensitive to the stress concentrations at the crack tips in the CEN specimen would have a fracture load given by

$$P_N = \frac{b - 2a}{b} P_0 \quad (10)$$

where P_0 is the unnotched failure load. On the other hand, if the material is brittle and has less tendency to accommodate a stress concentration, the notched strength P_N would fall below the prediction of Equation 10.

To investigate the notch sensitivity of the liner boards under consideration the non-dimensional notched strength, P_N/P_0, was measured at crack lengths $2a/b = 0.2$, 0.4 and 0.6.

Fig. 9 shows the experimental values for a 200 g m^{-2} liner board tested in the MD and CD, and the straight-line upper bound estimate provided by Equation 10. Experimental strengths fall below the linear relation for CEN specimens tested in both the MD and CD, illustrating that liner board is indeed crack-sensitive. The data points in the MD are lower than those in the CD at a given crack length, showing that the material is more ductile in the CD. Similar results were found for the 400 g m^{-2} liner board.

4.3. Fracture toughness determination

In this section the various methods of establishing the critical value of the J-integral, J_c, will be applied to the CEN data collected for the liner boards.

To obtain J_c^* with the MST a minimum of two crack lengths is required, because the area between two load–displacement curves is needed. In this study three crack lengths were studied, namely $2a/b = 0.2$, 0.4 and 0.6. Fig. 10 shows J^* calculated as a function of displacement for 200 g m^{-2} liner board in the MD and CD. These curves were obtained by first determining average load–displacement curves from ten replicates at a given crack length, and then integrating the difference between the load–displacement curves representing two consecutive crack lengths. The critical displacement required for J_c^* determination is here defined as the displacement at the point of maximum load for the longer crack. The J_c^* value so obtained is ascribed to an average crack length, e.g. the J_c^* evaluated from specimens with $2a/b = 0.2$ and 0.4 yields J_c^* for $2a/b = 0.3$. J_c^* was also reduced from the CEN data according to the SST and LNT as previously outlined. The shear modulus and Poisson's ratio required in Equation 4 were obtained from an approximate method proposed by Baum *et al.* [15] (see Appendix for more detail).

J_c^* obtained by the various methods are shown in Figs 11 to 14. The MST and LNT give similar J_c^* values that are independent of crack length. The SST gives larger toughness values than the MST and LNT.

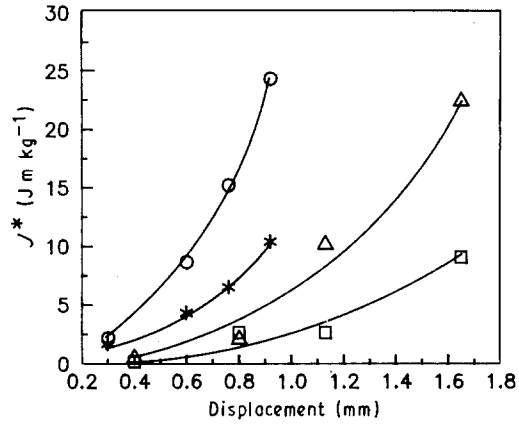

Figure 10 Specific J-integral against displacement for 200 g m^{-2} kraft liner evaluated by the multiple specimen method for crack length $2a/b$ of 0.2 to 0.4 (∗) in the MD and (□) in the CD, and 0.4 to 0.6 (○) in the MD and (△) in the CD.

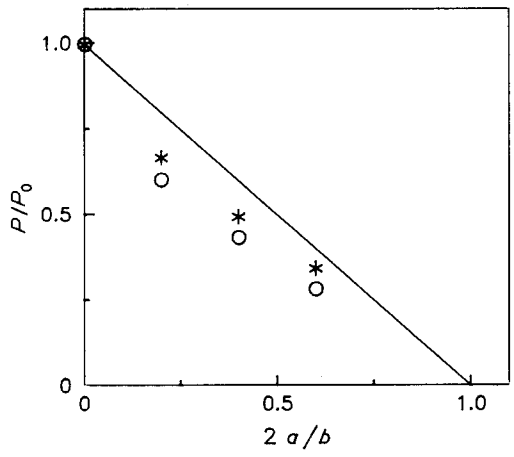

Figure 9 Notched strength P_N normalized with unnotched strength P_0 against crack length ($2a/b$) for 200 g m^{-2} kraft liner, (○) in the MD and (∗) in the CD.

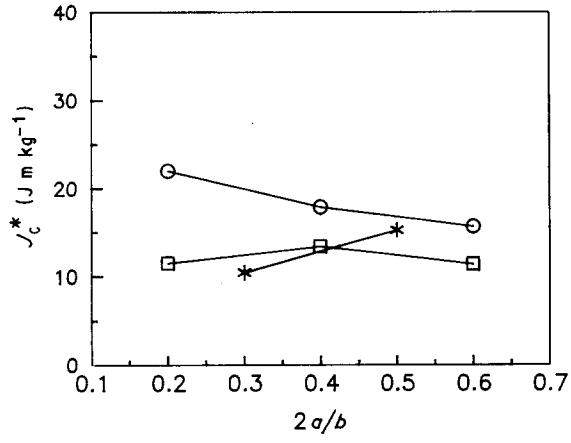

Figure 11 Specific fracture toughness J_c^* of kraft liner (200 g m^{-2}) in the MD against crack length. (∗) Multiple-specimen technique, (○) single-specimen technique, (□) Liebowitz non-linear technique.

TABLE II Elastic and plastic components of the specific J-integral for kraft liner in machine and cross direction

Grammage ($g\,m^{-2}$) and direction	Normalized crack length, $2a/b$	Multiple specimen J_c^* ($g\,m^{-2}$)	Single specimen			Liebowitz et al.		
			J_e^* ($J\,m\,kg^{-1}$)	J_p^* ($J\,m\,kg^{-1}$)	J_c^* ($J\,m\,kg^{-1}$)	J_e^* ($J\,m\,kg^{-1}$)	J_p^* ($J\,m\,kg^{-1}$)	J_c^* ($J\,m\,kg^{-1}$)
200, CD	0.2		2.7	36.4	39.1	2.7	6.1	8.8
	0.3	9.1						
	0.4		3.4	16.3	19.7	3.4	4.4	7.8
	0.5	10.2						
	0.6		3.4	10.3	13.7	3.4	2.9	6.3
200, MD	0.2		7.4	14.7	22.1	7.4	4.1	11.5
	0.3	10.5						
	0.4		9.0	8.9	17.9	9.0	4.4	13.4
	0.5	15.3						
	0.6		8.0	7.8	15.8	8.0	3.4	11.4
400, CD	0.2		3.2	40.9	44.1	3.2	6.9	10.1
	0.3	10.5						
	0.4		4.2	19.8	24.0	4.2	5.7	9.9
	0.5	8.5						
	0.6		4.4	13.6	18.0	4.4	4.6	9.0
400, MD	0.2		8.5	22.7	31.2	8.5	6.1	14.6
	0.3	13.5						
	0.4		10.7	13.4	24.1	10.7	5.0	15.7
	0.5	14.6						
	0.6		11.0	11.2	22.2	11.0	5.2	16.2

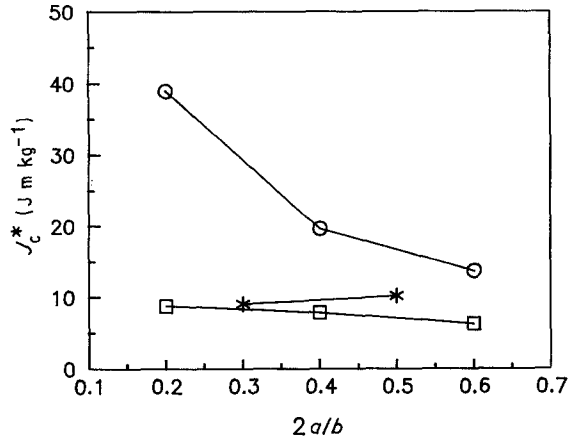

Figure 12 Specific fracture toughness J_c^* of kraft liner (200 $g\,m^{-2}$) in the CD against crack length. (*) Multiple-specimen technique, (○) single-specimen technique, (□) Liebowitz non-linear technique.

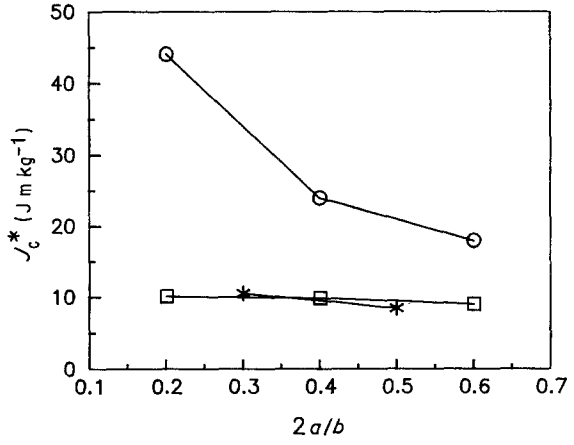

Figure 14 Specific fracture toughness J_c^* of kraft liner (400 $g\,m^{-2}$) in the CD against crack length. (*) Multiple-specimen technique, (○) single-specimen technique, (□) Liebowitz non-linear technique.

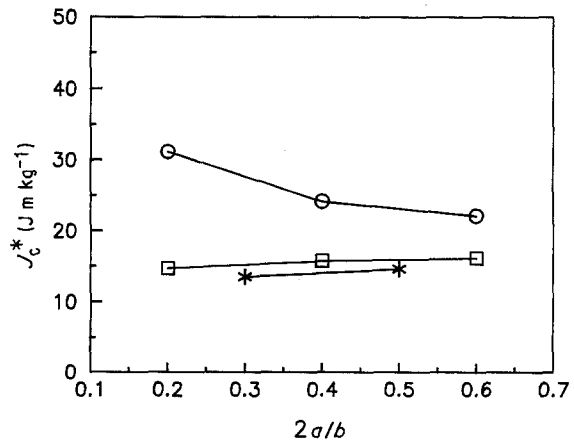

Figure 13 Specific fracture toughness J_c^* of kraft liner (400 $g\,m^{-2}$) in the MD against crack length. (*) Multiple-specimen technique, (○) single-specimen technique, (□) Liebowitz non-linear technique.

Furthermore, the toughness values show a strong dependency of crack length.

Table II provides data plotted in Figs 11 to 14 and the elastic and plastic components of the specific J-integral as determined by the SST and LNT. It is noted that the fraction of the plastic component is larger in the CD than in the MD. Most striking, however, is the significant disagreement between the plastic components of J_c^* obtained by the SST and LNT. While the LNT provides a plastic component of the same order of magnitude as the elastic component, the SST provides a plastic component which, in extreme cases, is an order of magnitude larger than the elastic part of J_c^*. This discrepancy is evidently a result of different modelling of the plastic part of the displacement in the SST and LNT.

Further inspection of the data in Table II reveals that the specific J-integral, J_c^*, is relatively independ-

ent of grammage and hence serves as a material-specific toughness parameter.

5. Conclusions

In this study three methods to evaluate the J-integral for liner board were presented and compared, based on their ability to provide consistent J_c^* values and on convenience. The three methods employed are the single-specimen, multiple-specimen and Liebowitz non-linear methods.

It was found that the single-specimen method yields a larger fracture toughness than the other methods. Moreover, the fracture toughness shows a large dependency on crack length. The multiple-specimen technique and Liebowitz non-linear method provide similar fracture toughness values that are independent of crack length. The Liebowitz method is, however, much easier to implement, based on amount of test data required and ease of data reduction methodology. This method shows, based on the limited results presented here, great promise for the experimental fracture toughness determination of paper.

Acknowledgements

One of the authors (L.A.C.) wishes to thank Dr A. de Ruvo, SCA Research, for providing funding to make this cooperative work possible. Dr de Ruvo also provided useful comments in the preparation of this manuscript.

APPENDIX: Approximation of shear modulus and Poisson ratios

Baum *et al.* [15] found that the in-plane shear modulus G_{xy} and Poisson ratios ν_{xy} and ν_{yx} for paper can be obtained approximately from the elastic moduli in machine and cross directions:

$$G_{xy} \approx 0.387(E_x E_y)^{1/2} \quad \text{(A1)}$$

$$(\nu_{xy}\nu_{yx})^{1/2} \approx 0.293 \quad \text{(A2)}$$

Furthermore, since paper is orthotropic the following relation is applicable [16]:

$$\nu_{xy}/E_x = \nu_{yx}/E_y \quad \text{(A3)}$$

Equations A2 and A3 combined give

$$\nu_{xy} \approx 0.293(E_x/E_y)^{1/2} \quad \text{(A4)}$$

References

1. D. BROEK, "Elementary Engineering Fracture Mechanics", 3rd Edn (Nijhoff, Dordrecht, 1984).
2. J. F. KNOTT, "Fundamentals of Fracture Mechanics" (Butterworths, London, 1973).
3. T. UESAKA, in "Handbook of Physical and Mechanical Testing of Paper and Paperboard", Vol. 1, edited by R. E. Mark (Dekker, New York, 1983) p. 77.
4. R. STEADMAN and C. FELLERS, paper presented at International Paper Physics Seminar, Minnowbrook, New York, August 1986.
5. *Idem*, paper presented at International Paper Physics Conference, Mont-Rolland, Canada, September 1987.
6. X. VOLOZINSKIS, PhD dissertation (in French), University of Bordeaux (1988).
7. J. R. RICE, *J. Appl. Mech.* **35** (1968) 379.
8. J. A. BEGLEY and J. D. LANDES, in "Fracture Toughness", ASTM STP 514 (American Society for Testing and Materials, Philadelphia, 1972) p. 1.
9. J. R. RICE, P. C. PARIS and J. G. MERKLE, in "Progress in Flaw Growth and Fracture Toughness Testing", ASTM STP 536 (American Society for Testing and Materials, Philadelphia, 1973) p. 231.
10. H. LIEBOWITZ and J. EFTIS, *Eng. Fract. Mech.* **3** (1971) 267.
11. J. EFTIS, D. L. JONES and H. LIEBOWITZ, *ibid.* **7** (1975) 491.
12. P. K. POULOSE, D. L. JONES and H. LIEBOWITZ, *ibid.* **17** (1983) 133.
13. C. FELLERS, H. ANDERSSON and H. HOLLMARK, in "Paper Structure and Properties", edited by J. A. Bristow and P. Kolseth (Dekker, New York, 1986) p. 151.
14. G. C. SIH, P. C. PARIS and G. R. IRWIN, *Int. J. Fract. Mech.* **1** (1965) 189.
15. G. A. BAUM, D. C. BRENNAN and C. C. HABEGER, *TAPPI* **64** (8) (1981) 97.
16. R. M. JONES, "Mechanics of Composite Materials" (Hemisphere, New York, 1975) p. 38.

Received 17 January
and accepted 2 August 1990